Modeling of contact between rough surfaces using homogenisation technique

Saoussen Belghith [a], Salah Mezlini [a,*], Hedi BelhadjSalah [a], Jean-Louis Ligier [b]

[a] *Laboratoire génie mécanique, École nationale d'ingénieurs de Monastir, 5000 Tunisia*
[b] *RENAULT S.A., Powertrain Engineering Division, rue des Bons Raisins, 92508 Rueil Malmaison, France*

A R T I C L E   I N F O

A B S T R A C T

In this study, microscopic deterministic and analytical contact models that take the properties of engineering surfaces into account have been developed. Geometrical characteristics of rough surfaces are deduced using the standard procedure for roughness and waviness parameters. These models allow the analyses of the asperities behaviour and real contact area. Comparison between the analytical and deterministic results shows a good correlation. The microscopic model is often enabling to simulate the real structure with complex geometry, so, a homogenisation technique has been developed. The interface of the equivalent model has been governed by the microscopic model results. Sensitivity of models responses to the random pulling of surfaces parameters has been also analysed.

1. Introduction

The topographies of interacting surfaces can have a significant influence on the global physical and mechanical behaviours of a technical system. There is, for example, a direct relation between the thermal and electromagnetic resistivity between interacting bodies and the real area of contact between the mating surfaces. In fact, real area results from the combination of the surface topography and geometry (roughness) with the mechanical behaviour of the asperities, which for metallic materials will undergo elastic, elastoplastic or plastic deformations, depending on their mechanical characteristics. So, resolving industrial problems requires often mechanical and topographic analyses at macroscopic and microscopic scale.

Many researchers have studied the microscopic behaviours of rough surfaces [1–3]. The first elastic contact model was developed by Greenwood and Williamson (GW) in 1966 [4]. This model represents the roughness by a number of hemispheres with the same curvature radius R and a Gaussian asperity height distribution. A relationship is found from the assumption that deformation is elastic (Hertz [5]), with no interaction between asperities during contact with a smooth rigid plan. The real contact area and the total force are expressed in terms of the distance separating the smooth surface and the mean plan of the rough surface. The GW model defines the plasticity index ψ:

$$\psi = \frac{E^*}{H} \sqrt{\frac{\sigma}{R}} \tag{1}$$

where E^* is the combined Young's modulus of the two surfaces, σ is the standard deviation of summit heights, R is the curvature radius, H is the hardness material. For moderate contact pressures, ψ indicates the average deformation mode of

---

* Corresponding author.
  E-mail address: salah.mezlini@laposte.net (S. Mezlini).

the rough surface. The deformation is elastic for $\psi < 0.6$, fully plastic for $\psi > 1$ and elastoplastic for $0.6 < \psi < 1$. However, contact area and mean pressure on each asperity are not known in the range of the plasticity index $0.6 < \psi < 1$.

Abbott and Firestone [6] built a model, where deformations of the asperities are taken to be entirely plastic. This model equates the contact between a rigid plan and the rough surface to the truncation of a surface by a plan. The real area is estimated to be a straightforward geometrical intersection of the plan and the rough surface. The contact pressure is given by the plastic flow pressure H of the rough surface.

Zahouani and Sidoroff [7] presented a method for the elastic–plastic analysis of this contact problem and showed that such approach can provide a significant understanding of the influence of the surface roughness upon the progressive development of the contact area under increasing normal load.

F. Robbe-Valloire et al. [8,9] determined a global load and real contact area at the contact of two rough surfaces for a given separation distance between them. Roughness has been described using probabilistic model based on the quantification of the variability in the summit altitude and the asperity radius. This model will be used in this work to compare numerical results of microscopic model. The Robbe-Valloire model has been taken because it gives not only a realistic description of the profile but also uses the concept of the sum surface.

In recent years, attempts were made to analyse contact of rough surfaces by means of numerical simulation. Among them there are works of Robert L. Jackson and Jeffery L. Streator [10] who describe a non-statistical multi-scale model of the normal contact between rough surfaces. The model considers the effect of having smaller asperities located on top of larger asperities in repeated fashion. Parameters describing the surface topography (asperity density and asperity radius) are calculated from an FFT performed of the surface profile. The model predicts a real contact area as a function of contact load. The limitation of this model is that the model assumes that all asperities at a given frequency behave identically in term of deformation, load support, etc.

R.S. Sayles [11] presented a numerical method using inversion approach. Real contact area in function of load has been compared with previous methods. A good agreement has been shown. He also presented distribution of rough surface pressure and the subsequent sub-surface stress effects they create. The numerical method has been applied to a two- and three-dimensional topography data.

M. Ciavarella et al. [12] studied a decrease of the elastic contact area in the elastic contact of fractal random surfaces when increasing roughness. They developed a numerical method using Fourrier and Weierstrass random series and involving a uniform distribution of pressure. Results of their method are compared with two recent models of Ciavarella [13] and Persson [14,15]. They show that both theories tend to underpredict the contact area.

D. Goerke and K. Willner [16] build a half space numerical model which describes the elastoplastic normal contact of isotropic fractal surfaces. Results of this numerical model are compared with experimental data which are obtained from contact tests of several aluminium specimens. The pressures versus gap curves were compared in both models. They show a good compliance except for small loads during unloading.

W. Everett Wilson et al. [17] developed a multiscale numerical model of rough surfaces to predict a real area of contact and surface separation as a function of load. Results of this model have been compared with existing statistical contact models. Comparison has shown qualitatively similar results. In accordance with concerns in previous works [10,13] that the iterative calculation of real contact area in multiscale methods does not converge, this work not only tests but also gives conditions required for convergence in these techniques.

More recently, B. Buchner et al. [18] developed a new concept based on a combination of the bearing area curve and a model asperity representing the average asperity slope of the original surface profile. The new approach allows the determination of the real contact area-load relation for any surface compressed by a flat tool without excessive effort. Comparison of the new concept calculations and the data obtained by simulating the upsetting of the original profile shows a good correspondence.

The aim of this Note is to analyse analytically the contact between rough surfaces and to simulate numerically a microscopic contact. Geometrical characteristics of rough surfaces are deduced from an experimental profile and using the standard procedure for roughness and waviness parameters (ISO12085) [19]. Comparison between deterministic and analytical studies has been discussed. The analytical model has been chosen because it allows on the one hand to take into account the roughness and waviness parameters and on the other hand to use the concept of the sum surface used in deterministic model. The evolution of real contact area and the sensitivity of the model response to the random pulling of the geometrical characteristics have been analysed.

Finally, an equivalent model based on the homogenisation technique has been presented. The interfacial behaviour of this model has been governed by the curve deduced from the microscopic model. The homogenisation technique has been validated by comparing the stress and strain states of the two models.

2. Analytical study

2.1. Microgeometry standard parameters (motif parameters)

This work is based on a standardised method [19] for determining the surface microgeometry. This description has already been used by F. Robbe-Valloire [20,21]. The measurements were performed with a classical stylus profile instrument
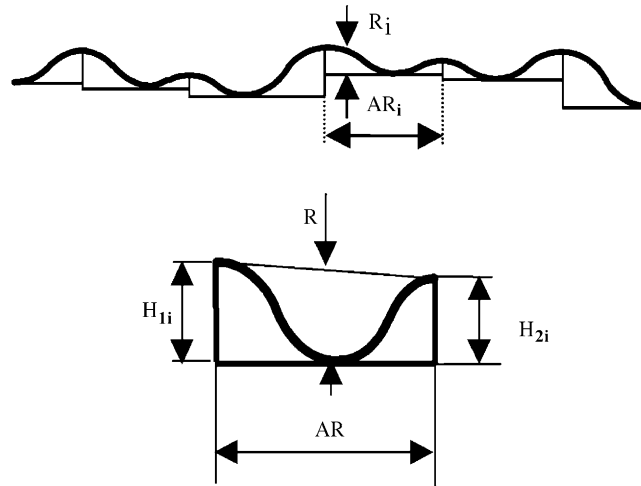
Fig. 1. Geometrical characteristics of a motif.

currently available on the commercial market. The obtained profile has been filtered, using a two-step procedure, into two profiles which successively provide roughness parameters and afterwards waviness parameters.

First the profile's main peak and valley are identified. Signal processing is obtained by means of a graphical method drawing upon the concept of a so-called "motif" defined as that part of the profile found between two peaks. The geometrical characteristics of the motif number i are as follows (Fig. 1):

- H_{1i} is the height between the left peak and the deepest valley;
- H_{2i} is the height between the right peak and the deepest valley;
- T_i is the smaller value of H_{1i} and H_{2i};
- R_i is the mean height (H_{1i}, H_{2i}) of the motif i;
- AR_i is the horizontal distance between the peaks of the motif i.

Four conditions have been used to combine or not two motifs. These conditions give the principal peaks and permit the calculation of roughness parameters:

- R is the average of the height values R_i of the motifs;
- AR is the average of the width values AR_i of the motifs;
- SR is the root mean square of the R_i values;
- SAR is the root mean square of the AR_i values.

With the motifs of roughness, it is possible to keep only the summits of the peaks and to reply the same methodology. This second step gives a new type of motif called a waviness motif. So, waviness parameters called W, AW, SW, and SAW have been obtained.

2.2. Description of the rough surfaces using Robbe-Valloire model

Greenwood and Williamson [4] introduced a statistical description in the variability of summit altitudes and proposed a curved shape of asperities with a constant radius.

Whitehouse and Archard [22] and Nayak [23] admit variation in asperity radius instead of merely in the summit altitudes.

This study describes asperity geometry by F. Robbe-Valloire's approach [8,9]. This approach assumed a perfect circular shape of asperities radius with a lognormal distribution. The mean radius of asperity is deduced from dimensional characteristics of each motif. The value is given by the following relation:

$$\rho_i = \frac{1}{16} \frac{AR_i^2}{H_i} \tag{2}$$

ρ_i changes from one asperity to another but it is possible to specify values of its variability.

The mean value ρ_m is expressed by:

$$\rho_m = \frac{1}{16} \frac{AR^2 + SAR^2}{R} \tag{3}$$

The associated root mean square value ρ_{rms} is given by:

$$\rho_{rms} = \frac{1}{16} \frac{AR^2}{R} \sqrt{\frac{SR^2}{R^2} + 4\frac{SAR^2}{AR^2}}$$ (4)

The distribution function of radius is

$$F(\rho^*) = \frac{1}{c_1 \rho^* \sqrt{2\pi}} \exp\left[-\frac{1}{2c_1^2}(\ln \rho^* - c_2)^2\right]$$ (5)

with

$$\rho^* = \frac{\rho}{\rho_{rms}}, \qquad c_1 = \sqrt{\ln\left(\frac{\rho_{rms}^2}{\rho_m^2} + 1\right)} \quad \text{and} \quad c_2 = \ln\left(\frac{\rho_m}{\rho_{rms}}\right) - \ln\left(\frac{\rho_{rms}^2}{\rho_m^2} + 1\right)$$

F. Robbe-Valloire assumes a normal distribution for the altitude of asperity summit. The mean value of summits altitude is $Z_m = 0$ and root mean square value is:

$$Z_{rms} = 0.35\sqrt{W^2 + SW^2}$$ (6)

The distribution function of summits altitude is:

$$f(z) = \frac{1}{Z_{rms}\sqrt{2\pi}} \exp\left[-\frac{1}{2}\left(\frac{Z - Z_m}{Z_{rms}}\right)^2\right]$$ (7)

2.3. Analysis of the contact between two rough surfaces

In this study, we transform the contact between rough deformable surfaces into the contact between a smooth rigid surface and a rough deformable which is called sum surface. Microgeometry and mechanical characteristics of the sum surface are deduced from each surface in contact.

- Microgeometry of the sum surface
  The microgeometry parameters of the sum surface results from parameters of each surface in contact. Thus, the following relations give microgeometric parameters of the sum surface from parameters of each surface in contact:

$$R = R_1 + R_2 \quad \text{and} \quad W = W_1 + W_2$$ (8)

$$SR = \sqrt{SR_1^2 + SR_2^2} \quad \text{and} \quad SW = \sqrt{SW_1^2 + SW_2^2}$$ (9)

$$AR = \frac{1}{2}(AR_1 + AR_2) \quad \text{and} \quad AW = \frac{1}{2}(AW_1 + AW_2)$$ (10)

$$SAR = \sqrt{SAR_1^2 + SAR_2^2} \quad \text{and} \quad SAW = \sqrt{SAW_1^2 + SAW_2^2}$$ (11)

- Mechanical characteristics of the sum surface
  – Elasticity of the sum surface
    Young's modulus is deduced from Young's modulus of each surface in contact using a classical relation:

$$\frac{1}{Eq} = \frac{1}{2}\left(\frac{1 - \nu_1^2}{E_1} + \frac{1 - \nu_2^2}{E_2}\right)$$ (12)

  – Plasticity of the sum surface
    The yield stress of the material constituting the sum surface corresponds to the lowest value of the yield stress of each surface in contact.

2.4. Results

2.4.1. Description of the simulated contact

Profiles of the two rough studied surfaces 1 and 2 are presented in Fig. 2. These geometrical characteristics are deduced using the standard procedure previously described. The microgeometrical parameters of the sum surface are also calculated using the previous relationship (Table 1).

The two surfaces 1 and 2 have a Poisson ratio of $\nu = 0.3$ and respectively Young's module of 60 and 68 GPa. So, the material of the sum surface has the following properties: Young's module: $E = 70$ GPa, Poisson ratio: $\nu = 0.3$ and yield stress of the material: $R_{pe} = 38$ MPa. The apparent contact area is $A_0 = 3.8$ mm.
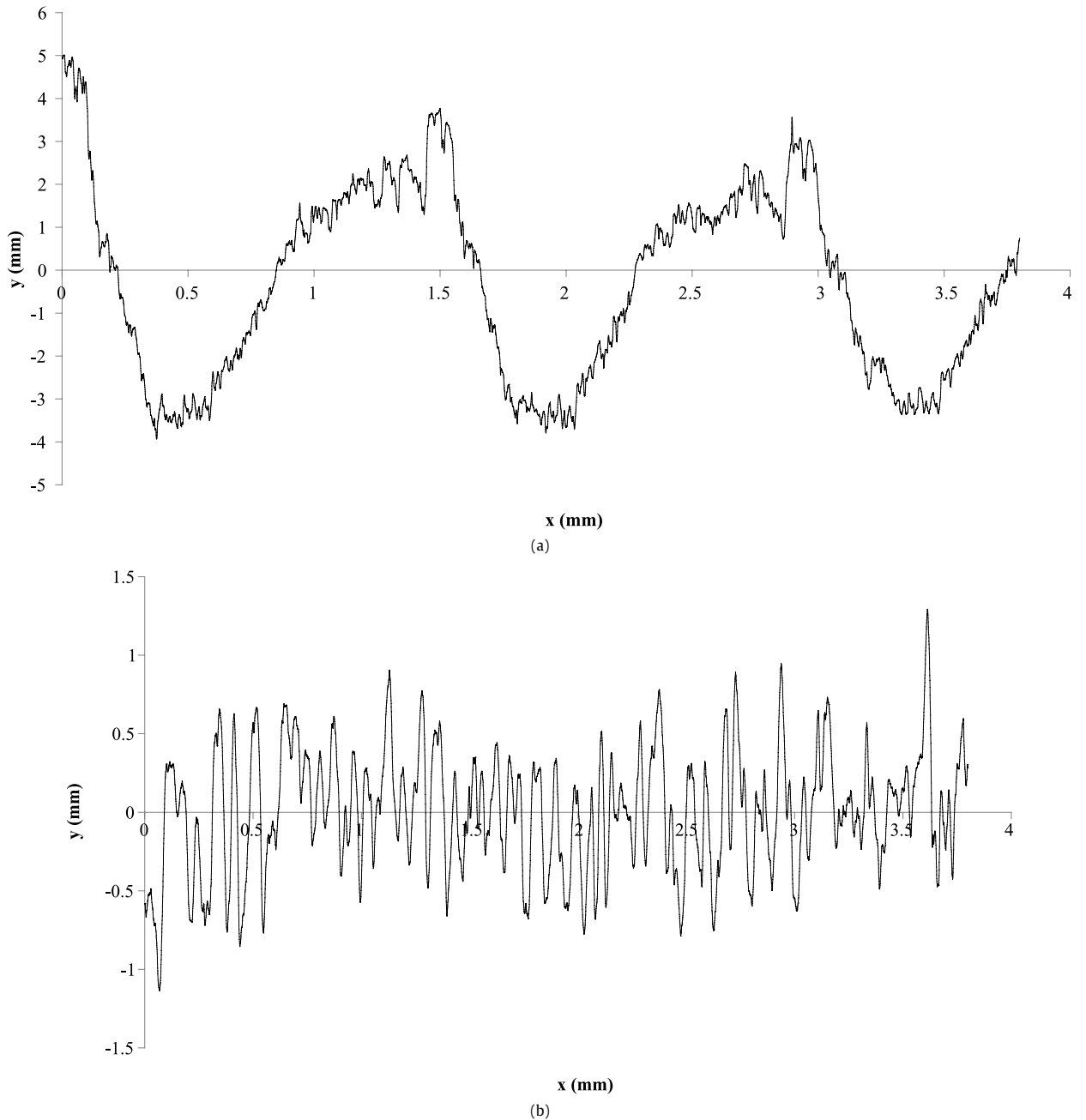
Fig. 2. Profiles of the contacting surfaces: (a) surface 1, (b) surface 2.

2.4.2. Normal load transmitted by contact

Because of the variability of summit altitude and radius of the asperities, we take the two parameters as variables. Three classical stages of deformation have been considered: elastic, elastoplastic and plastic. The position "*d*" of the smooth and rigid surface from the mean line of summits altitude of the rough and deformable surface has been also defined (Fig. 3).

Thus, local contact can occur only on the asperities having a summit altitude Z exceeding "*d*". Such asperities are deformed by interference $\delta = Z - d$.

In order to determine the normal forces transmitted through elastic, elastoplastic and plastic asperities the following relations have been used [8,9]:

Table 1
Microgeometrical parameters of the rough surface

	Surface 1	Surface 2	Sum surface
R (µm)	1.13	2.05	3.19
SR (µm)	0.27	0.76	0.81
AR (µm)	137	177	157
SAR (µm)	63	105	122
W (µm)	0.47	6.45	6.92
SW (µm)	0.07	0.83	0.84
AW (µm)	654	1299	976
SAW (µm)	122	256	284
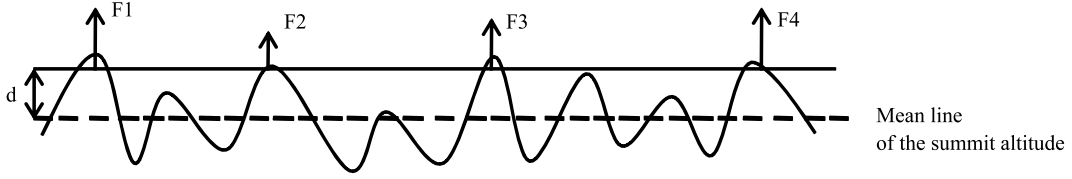
Fig. 3. Schematic description of the distance between the two surfaces.

$$Q_{elast} = 1.2 \frac{A_0}{AR^2} \int_{z=d}^{Z_{max}} \int_{\rho_e}^{\rho_{max}} W_1 f(z) F(\rho) \, dZ \, d\rho \tag{13}$$

$$Q_{elastoplast} = 1.2 \frac{A_0}{AR^2} \int_{z=d}^{Z_{max}} \int_{\rho_{ep}}^{\rho_e} W_2 f(z) F(\rho) \, dZ \, d\rho \tag{14}$$

$$Q_{plast} = 1.2 \frac{A_0}{AR^2} \int_{z=d}^{Z_{max}} \int_{0}^{\rho_{ep}} W_3 f(z) F(\rho) \, dZ \, d\rho \tag{15}$$

with:

$$W_1 = \frac{2}{3} \left(\delta^3 E_q^2 \rho \right)^{1/2}$$

$$W_2 = \frac{2\pi}{3} \rho (2\delta - \delta_e) R_{pe} \left[1.8 + \ln \left(\frac{1}{6} \frac{E_q}{R_{pe}} \frac{\sqrt{\rho(2\delta - \delta_e)}}{\rho} \right) \right]$$

$$W_3 = 3\pi \rho (2\delta - \delta_e) R_{pe}$$

$$\rho_e = \left(\frac{\delta}{27.4} \right) \left(\frac{E_q}{R_{pe}} \right)^2, \qquad \rho_{ep} = \left(\frac{\delta}{3976} \right) \left(\frac{E_q}{R_{pe}} \right)^2$$

z_{max} and ρ_{max} are the maximum values for altitude and the radius of asperities on a given surface. The global load on the contact is given by:

$$Q = Q_{elast} + Q_{elastoplast} + Q_{plast}$$

Fig. 4 shows the evolution of the apparent contact pressure $\frac{Q}{A_0}$ with the distance "d" separating surfaces. Apparent contact pressure in this case increases from 0 to 47 MPa which corresponds in a total crush of asperities above the mean line of the summits altitude.

2.4.3. Cumulative area of contact

It is possible to obtain the real area of contact transmitted by the normal load through the three stages of deformations using the following expressions:

$$A_{elast}(d) = 1.2 \frac{A_0}{AR^2} \int_{z=d}^{Z_{max}} \int_{\rho_e}^{\rho_{max}} \pi (z - d) \rho f(z) F(\rho) \, dZ \, d\rho \tag{16}$$
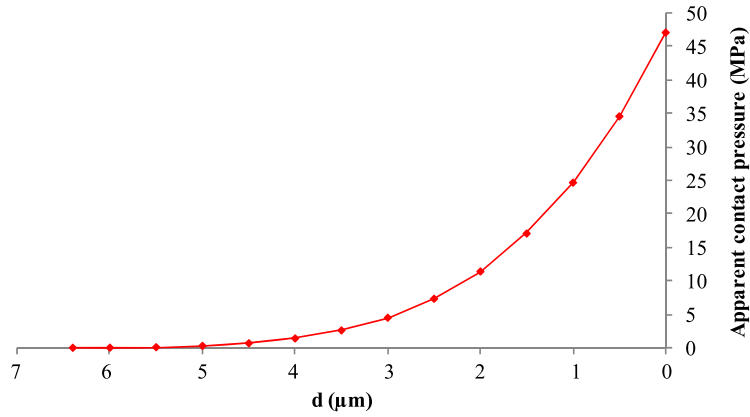
Fig. 4. Evolution of apparent contact pressure as a function of the distance "d".
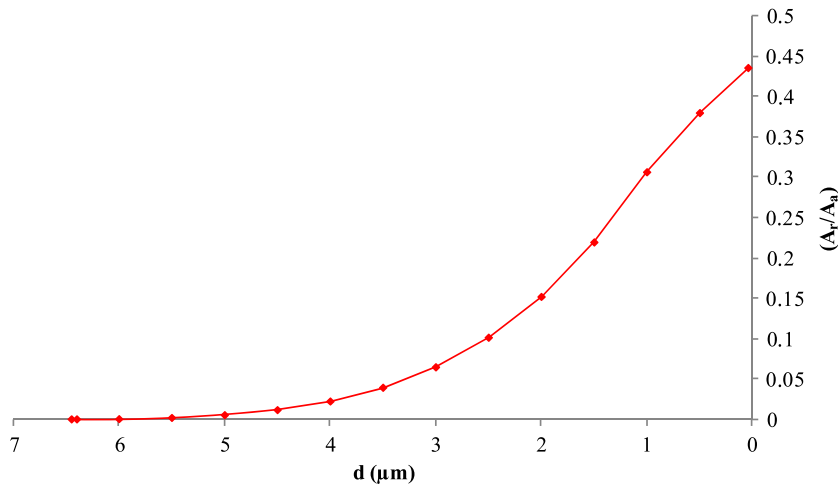
Fig. 5. Evolution of the ratio A_r/A_a in function of the mean separation distance.

$$A_{elastoplast}(d) = 1.2 \frac{A_0}{AR^2} \int\limits_{z=d}^{Z_{max}} \int\limits_{\rho_{ep}}^{\rho_e} \pi \left[2(z-d) - \delta_e\right] \rho f(z) F(\rho) \, dZ \, d\rho \tag{17}$$

$$A_{plast}(d) = 1.2 \frac{A_0}{AR^2} \int\limits_{z=d}^{Z_{max}} \int\limits_{0}^{\rho_{ep}} \pi \left[2(z-d) - \delta_e\right] \rho f(z) F(\rho) \, dZ \, d\rho \tag{18}$$

Thus, the real contact area is:

$$A_r(d) = A_{elast}(d) + A_{elastoplastic}(d) + A_{plastic}(d)$$

Fig. 5 illustrates the evolution of the ratio of the real contact area to the apparent contact area in function of separation distance "d". The ratio A_r/A_a increases when the distance "d" decreases.

3. Deterministic microscopic model

3.1. Deterministic model

As described previously the contact between two rough surfaces is transformed to the contact between a rough surface and a perfectly smooth plan. The material's behaviour of the rough surface is modulated using large deformation and elastoplastic theory. More specifically, the plastic flow is described via the Von Mises plasticity criterion. The material's characteristics used previously have been taken (Young modulus of 70 GPa, a Poisson ratio of 0.3 and a constant yield stress σ_{pe} of 38 MPa). A non-linear elastoplastic behaviour has been used (Fig. 6).
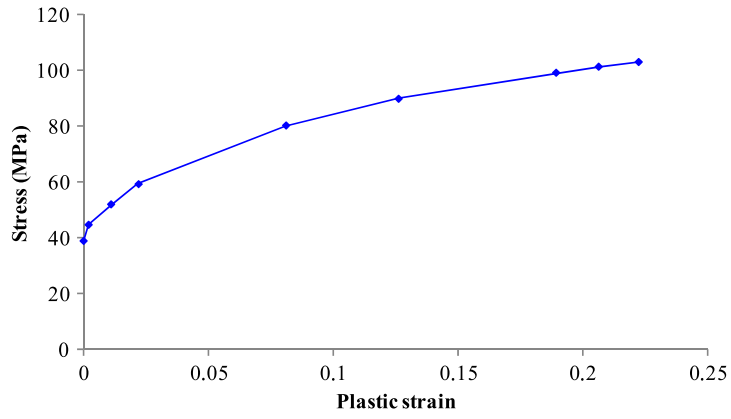
Fig. 6. Stress–strain hardening curve.
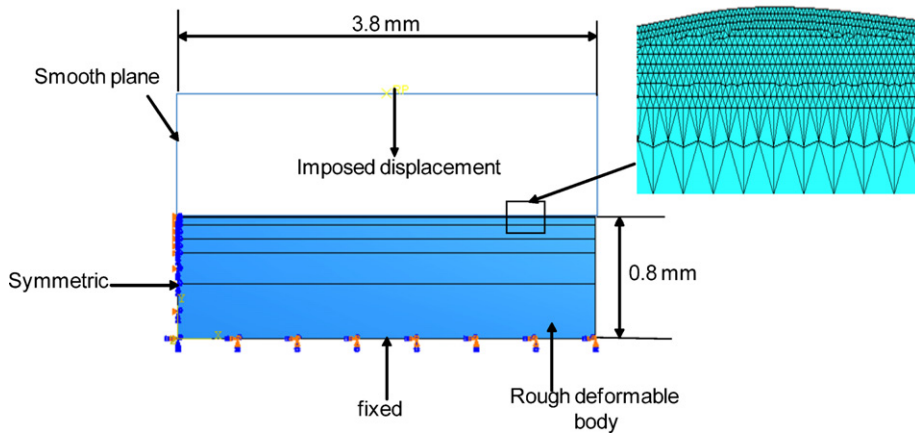
Fig. 7. Boundary conditions, dimensions and mesh used in numerical simulation.
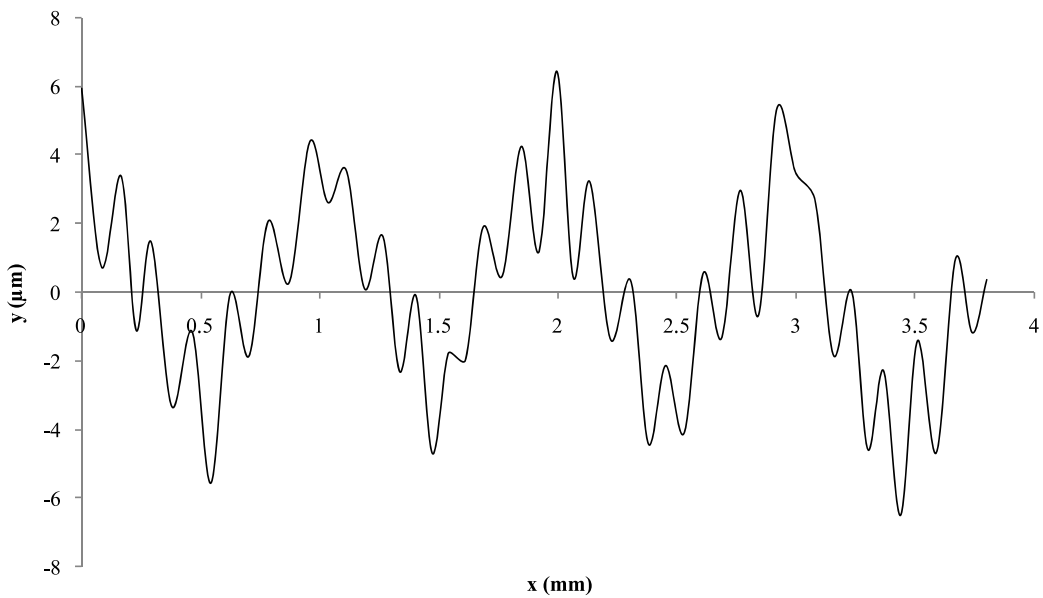
Fig. 8. Profile of the sum surface.
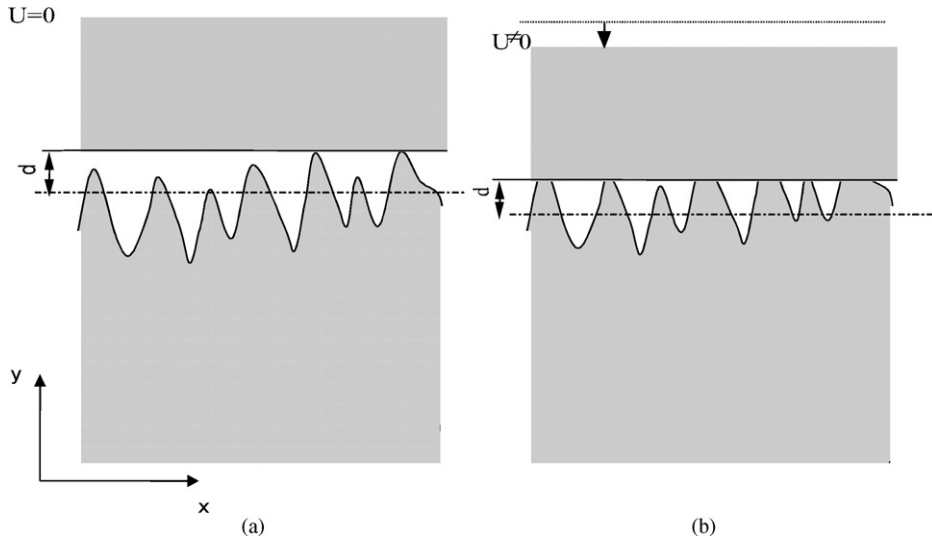
Fig. 9. Distance between the rigid plane and the mean line profile for different displacements: (a) $u = 0$, (b) $u \neq 0$.
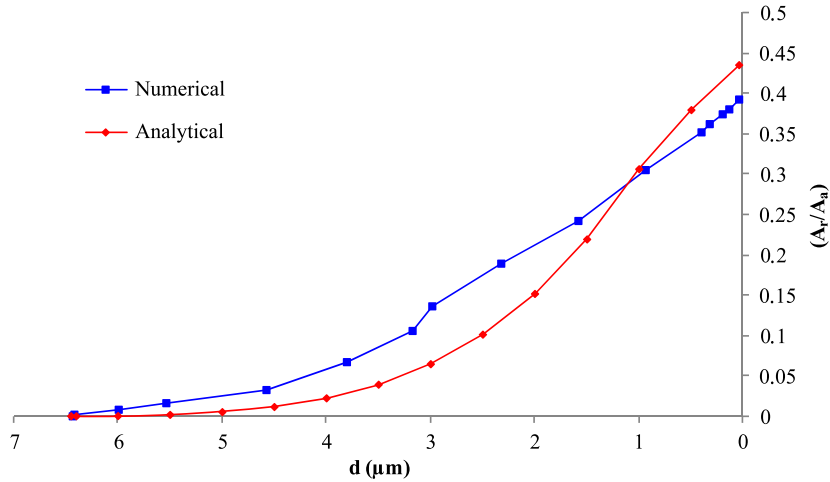
Fig. 10. Evolution of the ratio A_r/A_a with the distance "d" for analytical and numerical models.

2D model has been used using ABAQUS/Standard. The width of the two contacting bodies is 3.8 mm. The height of the smooth rigid body is 1 mm and height of the deformable rough body is 0.8 mm. Free mesh types have been considered. They are particularly refined near the interface having a size between 3 and 5 µm, but are sufficiently large away from the rough surface having a size of 100 µm. Dimensions and boundary conditions of the model are shown in Fig. 7. Loading is achieved by monitoring the smooth and rigid plan quasi-static displacement (dynamic effects are neglected), which is pushed vertically into the volume to investigate the crushing.

In this model, the same roughness and waviness parameters of the sum surface have been considered. A Matlab program has been developed in order to obtain coordinates of summits and valleys of the sum surface profile from roughness and waviness parameters presented in Table 1. This program allows the regeneration of both the waviness and roughness profiles while assuming that waviness and roughness parameters have a lognormal distribution. The surface profile has been obtained using a superposition of the roughness profile upon the waviness one.

The summits and valleys coordinates of this profile have been introduced in the 2D numerical model using python scripts. Afterwards, they have been interpolated by splines. Fig. 8 showed a simulated profile.

In order to evaluate the real contact area, nodes of a rough surface which have a contact with the rigid body have been obtained. So, to verify if a node is in contact or not with the rigid, contact pressure relative to surface nodes has been controlled. The node is in contact with the rigid, if the pressure is different from zero. Real contact area has been deduced for several increments relative to different values of the distance "d" separating contacting surfaces (Fig. 9).

Fig. 10 presents analytical and deterministic results of the evolution of the ratio A_r/A_a with the distance "d". The deterministic and analytical curves have the same tendency and the maximum relative error between two models is 9%.
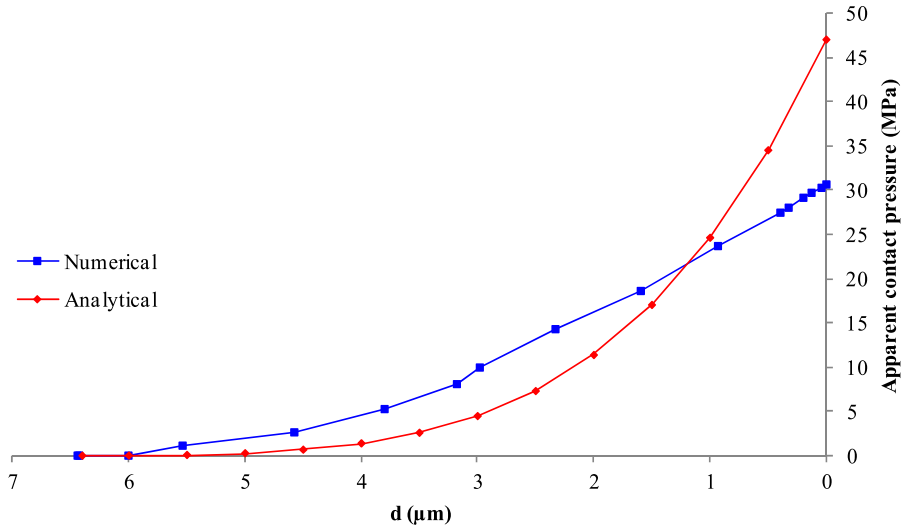
Fig. 11. Evolution of the apparent contact pressure as a function of the distances "*d*" for analytical and numerical models.
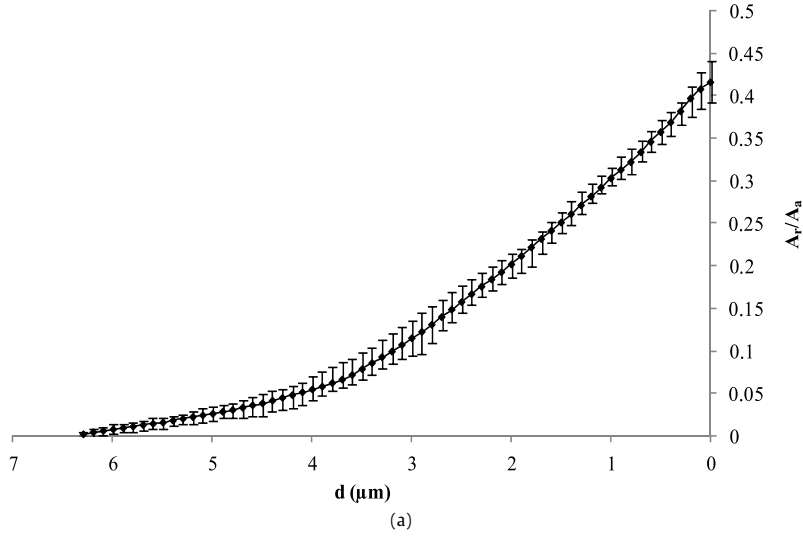
(a)
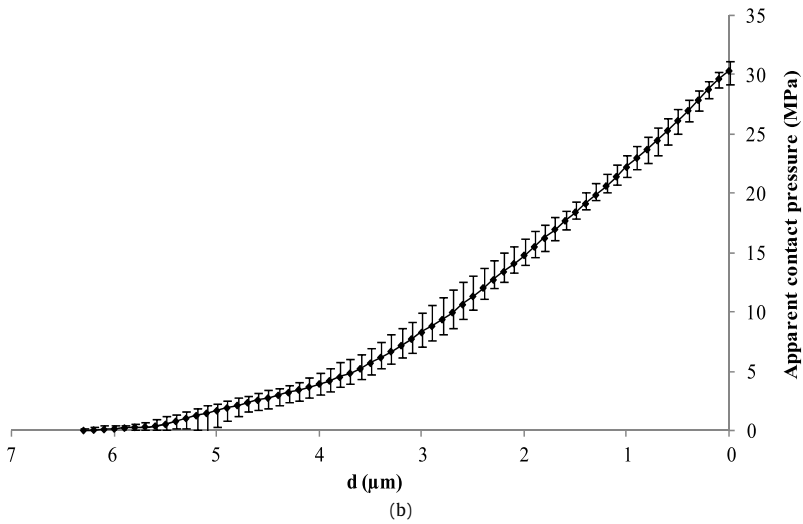
(b)

Fig. 12. Sensitivity of the model responses to the random pulling of roughness parameters (10 pullings): (a) A_r/A_a, (b) apparent contact pressure.
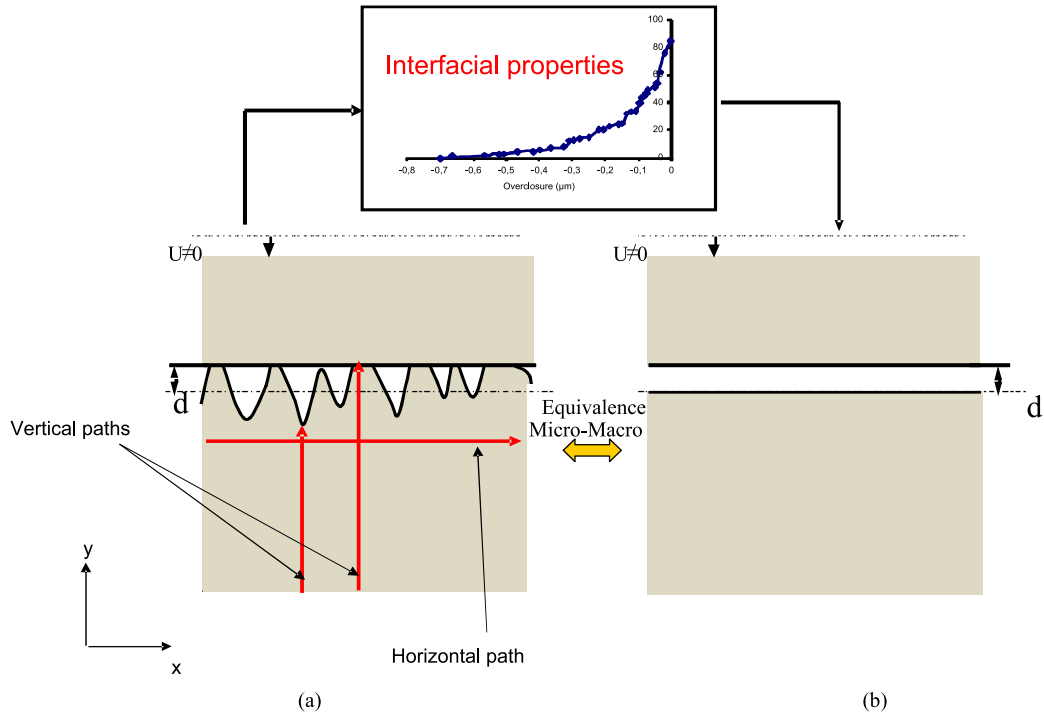
Fig. 13. Schematic representation of micro–macro scale: (a) micro, (b) macro.

The apparent contact pressure has also been analysed. Fig. 11 presents the analytical and deterministic results of the evolution of the apparent contact pressure as a function of the distance "d". It shows that for the two models the apparent contact pressure increases by decreasing the distance "d".

The difference between the two models is essentially due to the difference between assumptions. In fact, in the analytical model, the spherical asperities have been considered. However, in the deterministic model, summits have been related using splines. Moreover, in the deterministic model, the elastoplastic behaviour and interaction between asperities have been taken into account.

3.2. Sensitivity of the model response to random pulling of the profile parameters

The previous results have been obtained for one random pulling of the roughness and waviness parameters (R, SR, AR, SAR, W, SW, AW and SAW). Therefore, the study of the effect of the random pulling on the response of the deterministic model is important. The evolution of the ratio (A_r/A_a) and apparent contact pressure with the separation distance surfaces for 10 arbitrary pulling of the roughness profile has been analysed. Fig. 12 illustrates the dispersion of these evolutions with the distance "d". It shows that the model response depends on the random pulling. This dispersion can govern the evolution of deformation modes of asperities as well as some physical properties such as thermal contact resistance.

4. Deterministic equivalent model

4.1. Homogenisation technique

In the industrial cases, real structures with large dimensions have been often used. Therefore, taking into account the topographic rough surfaces of these structures becomes complex and the numerical generation of the profile of large dimension surfaces is difficult and the computing time becomes very important.

So, it is necessary to build a macroscopic equivalent model which allows on the one hand to simulate the real large dimension structures and on the other hand, to take into account the effect of the rough contact surfaces.

We propose in this work to set up a methodology allowing studying the macroscopic scale analyses based on the microscopic results. The strategy suggested considers that the interfacial behaviour of the equivalent model has been governed by the synthesis curve (apparent contact pressure–separation distance) deduced from the microscopic model (Fig. 13).

The same boundary conditions of the microscopic model have been used. Quadrangular elements have been used and the meshes are particularly refined near the rough surface.
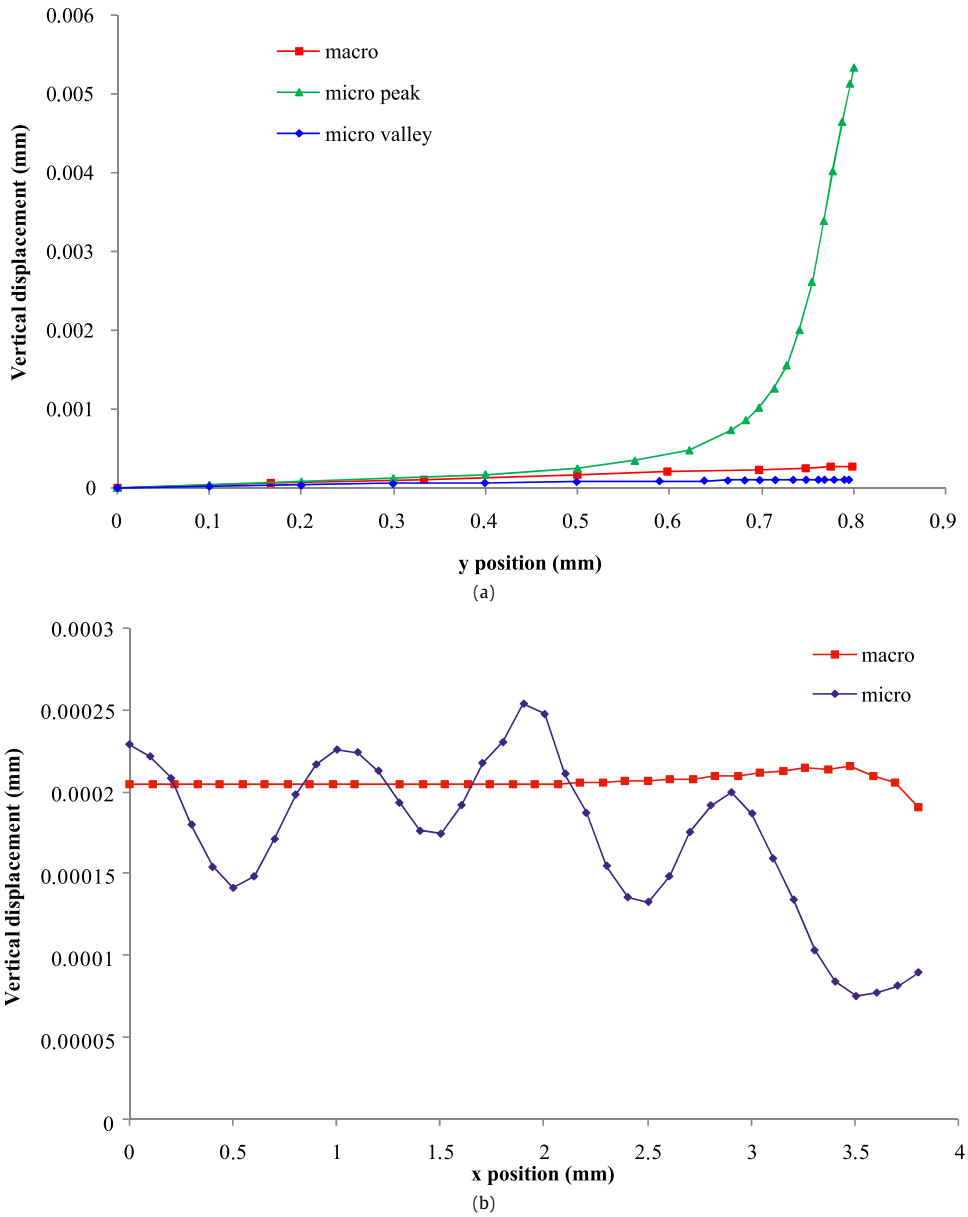
Fig. 14. Vertical displacement for $F = 100$ N and relative to microscopic and equivalent model with the: (a) y position, (b) x position.

4.2. Validation of homogenisation technique

The correlation between microscopic and the equivalent model has been studied using a comparison between stress and strain (displacement) relative to different horizontal and vertical paths. Two vertical and one horizontal path have been considered for the microscopic model (Fig. 13). The first vertical path is relative to a peak; however, the second corresponds to a valley. The horizontal path has been considered at 1/3 of depth away from the rough surface. Equivalent paths have been considered for the equivalent model. Vertical and horizontal (at 1/3 of depth) paths of equivalent model have also been considered.

Displacements relative to the different vertical and horizontal paths have been illustrated respectively in Figs. 14a and 14b. These displacements have been obtained for a relatively low normal load (100 N). Fig. 14a shows that near to the fixed base, the difference between displacements of two models is not significant. However, near to the rough surface, this difference becomes more important. This behaviour is governed essentially by the presence of the asperities in the interface. Fig. 14a shows also that the displacement in the peak is larger than the one of the valley. In fact, during the beginning of the loading, contact has occurred in the peaks and therefore they are more loaded.
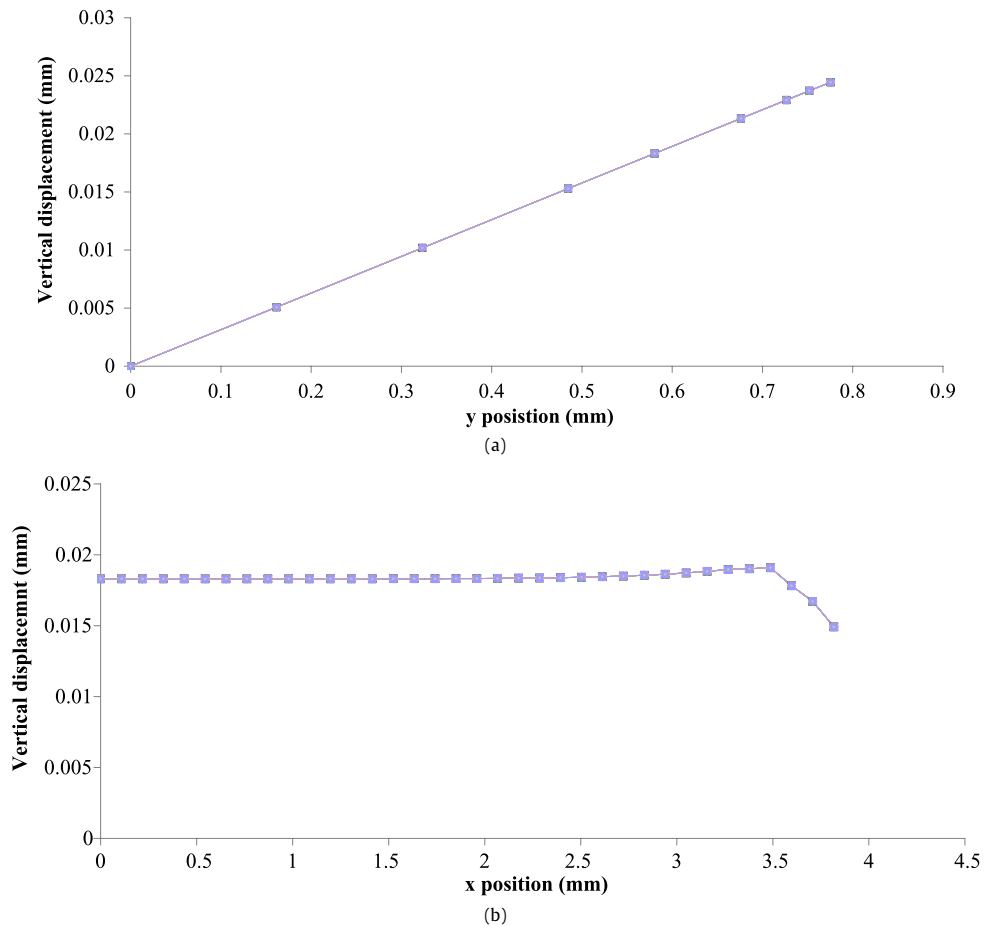
Fig. 15. Vertical displacement relative to equivalent model for 10 interfacial curves as a function of: (a) *y* position, (b) *x* position.

The vertical displacement relative to the horizontal path at 0.53 mm from the bottom surface has been also analysed. Fig. 14b presents the results relative to microscopic and equivalent model. It shows that the microscopic path presents more fluctuation than the equivalent one. This fluctuation is due to the presence of the asperities in the rough surface of microscopic model.

The same analysis has been investigated for a larger normal load ($F = 284$ N). It shows that the path disturbance near the rough surface is less than these obtained in the previous case.

4.3. Sensitivity of the equivalent model response to the random pulling of the profile parameters

Sensitivity of the equivalent model response to the random pulling of microscopic profile of the surface has been analysed. Fig. 15 illustrates the evolution of vertical displacement relative to the vertical and horizontal paths for a normal load $F = 450$ N which corresponds to a final increment of the analysis. These displacements have been obtained using 10 curves of interfacial microscopic model which correspond to 10 pullings of the profile. It shows that there is no difference between results. We deduce that the equivalent model is not sensitive to random pulling of the profile of the microscopic model.

5. Conclusion

In this study, contact between rough deformable surface and rigid smooth plan has been investigated. Microscopic and equivalent macroscopic models have been developed. Roughness parameters for the microscopic model were deduced using the standard procedure for roughness and waviness parameters ISO12085. Elastoplastic behaviour of the rough surface allows taking into account the different deformation modes of asperities. This model allows also analysing the real contact area with the distance separating surfaces. Results of deterministic microscopic model have been validated with an analytical study and a good correlation is found. The deterministic model responses are not very sensitive to the random pulling of the different parameters.

An equivalent model using a homogenisation technique has also been developed. This model makes it possible to simulate complex and large-sized structures while taking into account the topographic characteristics. The interfaces in the

equivalent model have been governed by a synthesis curve deduced from the microscopic model. The validation of the homogenisation technique was also carried out through the analysis of the displacement states. The sensitivity of the equivalent model to the random pulling of the microscopic profile has been also realised.

References

[1] D. Tabor, The Hardness of Metals, Oxford University Press, 1951.
[2] K.L. Johnson, Contact Mechanics, Cambridge University Press, 1985.
[3] M. Ciavarella, J.A. Greenwood, M. Paggi, Inclusion of "interaction" in the Greenwood and Williamson contact theory, Wear 265 (2008) 729–734.
[4] J.A. Greenwood, J.B.P. Williamson, Contact of nominally flat rough surfaces, Proc. R. Soc. A 295 (1966) 300–319.
[5] H. Hertz, On the elastic contact of elastic solids, J. Reine Angew. Math. 92 (1881) 156–171.
[6] E.J. Abbott, F.A. Firestone, Specifying surface quality – A method based on accurate measurement and comparison, Mech. Eng. 55 (1933) 569.
[7] H. Zahouani, F. Sidoroff, Rough surfaces and elastoplastic contact, C. R. Acad. Sci. Paris 2 (4) (2001) 709–715.
[8] F. Robbe-Valloire, R. Progri, B. Paffoni, R. Gras, Modélisation de la topographie microgéometrique Application à l'écrasement de surfaces, Matériaux et techniques 3–4 (2000) 33–40.
[9] F. Robbe-Valloire, B. Paffoni, R. Progri, Load transmission by elastic, elasto-plastic or fully plastic deformation of rough interface asperities, Mech. Mater. (2001) 617–633.
[10] Robert L. Jackson, Jeffery L. Streator, A multi-scale model for contact between rough surfaces, Wear 261 (2006) 1337–1347.
[11] R.S. Sayles, Basic principles of rough surface contact analysis using numerical methods, Tribol. Int. 29 (8) (1996) 639–650.
[12] M. Ciavarella, C. Murolo, G. Demelio, On elastic contact of rough surfaces: Numerical experiments and comparisons with recent theories, Wear 261 (2006) 1102–1113.
[13] M. Ciavarella, G. Demelio, J.R. Barber, Y.H. Jang, Linear elastic contact of the Weierstrass profile, Proc. R. Soc. London A 456 (2000) 387–405.
[14] B.N.J. Persson, Theory of rubber friction and contact mechanics, J. Chem. Phys. 115 (8) (2001) 3840–3861.
[15] B.N.J. Persson, Elastoplastic contact between randomly rough surfaces, Phys. Rev. Lett. 87 (11) (2001), art. No. 116101.
[16] D. Goerke, K. Willner, Normal contact of fractal surfaces – Experimental and numerical investigations, Wear 264 (2008) 589–598.
[17] W. Everett Wilson, Santosh V. Angadi, Robert L. Jakson, Surface separation and contact resistance considering sinusoidal elastic–plastic multi-scale rough surface contact, Wear 268 (1–2) (January 2010) 190–201.
[18] B. Buchner, M. Buchner, B. Buchmayr, Determination of the real area for numerical simulation, Tribol. Int. 42 (2009) 897–901.
[19] International Organisation for Standardisation (ISO), NF EN ISO 12085 (1988), Spécifications géométriques des produits – Méthode du profil – Paramètres liés aux motifs.
[20] F. Robbe-Valloire, Statistical analysis of asperities on a rough surface, Wear 249 (2001) 401–408.
[21] F. Robbe-Valloire, Approche stochastique de l'analyse du contact statique entre surfaces rugueuses, Tribologie et conception mécanique, Saint-Ouen, 2004, pp. 155–165.
[22] D.J. Whitehouse, J.F. Archard, The properties of random surfaces of significance in their contact, Proc. R. Soc. 316 (1970) 97–121.
[23] P.R. Nayak, Random process model of rough surfaces, Journal of Lubrification Technology 93F (1971) 398–407.